Available online at www.sciencedirect.com
SCIENCE DIRECT®
Optics & Laser Technology 37 (2004) 9–20
Optics & Laser Technology
www.elsevier.com/locate/optlastec

Limit analysis for laser removal of micron contaminant colloidal silicon dioxide particles from the super-smooth optical glass substrate by pulse Nd:YAG laser

Meng Hua[a,*], Xingkuan Shi[a,b], Edmund Cheung[a], Weizheng Yuan[b]

[a] *Department of Manufacturing Engineering and Engineering Management, City University of Hong Kong, 83 Tat Chee Avenue, Kowloon Tong, Hong Kong*
[b] *Department of Aircraft Manufacturing Engineering, Northwestern Polytechnical University, Xi'an Shaanxi 710072, PR China*

Received 10 September 2002; received in revised form 11 October 2003; accepted 4 February 2004

Abstract

Multimode Nd:YAG pulse laser was applied to remove micron and submicron particles by vaporizing a thin paint film pre-coated on super-smooth optical substrate surface. By analyzing the poor absorption of the optical glass substrate to the irradiative Nd:YAG pulse laser, the removal mechanism of contaminated colloidal particles from the super-smooth surface through vaporization of a volatile solid film is described. A limit analysis was proposed to determine the lower and the upper threshold of laser fluence for cleaning the SiO_2 contaminants from super-smooth K8 optical substrate. Relevant experiments on laser cleaning of micron-polishing particles from super-smooth K8 optical substrate confirmed the usefulness of this method in assisting the selection of effective cleaning fluence for accomplishing high cleanliness, which was in a range of 80–90% of the predicted upper threshold.

Keywords: Super-smooth substrate surface; Laser cleaning; Micro-particle contamination; Nd:YAG laser

1. Introduction

Surface cleaning is an important branch of surface engineering. Although there exist numerous processes in cleaning optical substrate surface, the individual processes have their respective limitations. Typically, plasma cleaning is susceptible to damaging surface and impractical for removing residues from high-performance surfaces, while water jet spray cleaning has unsatisfactory efficiency [1–3]. Most of these techniques involve the use of chemical and aqueous solutions [3,4].

Majority of current techniques for cleaning optical surface are largely associated with chemical–mechanical supersonic or megasonic processes [2,5,6], which are generally very complicated and difficult to remove micro-particles. The use of chemical solutions or solvents in cleaning [4] may cause etching effect and thus damage the surface of substrate material, thus fatally jeopardizing the quality and reliability of the high-performance optics and components in their service life [7]. Furthermore, micro- or sub-micro-contaminants on the substrate may also cause the problems of light diffusion, scattering, refraction and reflection. Consequently, the surface integrity, the structure and physical characteristics of the substrate are degraded, which badly influences the successful transmission of light or some special characteristics of a coated film. Laser cleaning method [8–15] subsequently emerges as an alternative approach to overcome the above-mentioned setbacks for removal of these harmful and tiny contaminant particles from an optical and super-smooth substrate. There are fundamentally two distinguishing approaches, respectively, dry and steam laser cleaning, for removing particles from solid substrate using laser as propounded in the available literature [9,11–14]. The dry laser cleaning approach merely involves with the incidence of laser beam directly onto low melting temperature contaminants adhering on the surface so as to evaporate them. The steam approach is normally associated with the application of an assisting liquid film onto the cleaning surface for removing substances, and the cleaning of high melting-point temperature substances occurs only by the thrust action of the evaporating liquid film.

* Corresponding author. Tel.: +852-2788-8443; fax: +852-2788-8423.
E-mail address: memnghua@cityu.edu.hk (M. Hua).

0030-3992/$ - see front matter © 2004 Elsevier Ltd. All rights reserved.
doi:10.1016/j.optlastec.2004.02.004

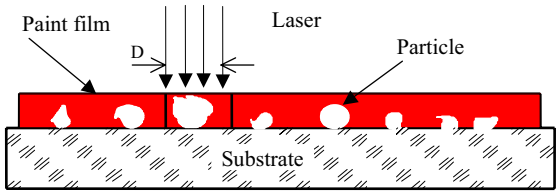

Fig. 1. Physical model of laser cleaning.

To remove particles from the surface of various solid substrates [12–14] like silicon and silicon carbide, magnetic head, aluminum oxide, lithography membrane mask, metal (i.e. aluminum, tin and copper), and quartz, etc., using laser, Lu et al. [13,14] have found that the cleaning efficiency varies with the laser fluence, the absorptivity to the pulsed laser radiation of the particles, and the substrate surface. The theoretical models that they established [12–14] for laser removing particles from the solid surfaces were merely for substrate surfaces or removing particles having good absorptivity to laser. Their models fail to provide useful prediction when both substrates and contaminant particles are transparent and have poor absorptivity to laser. Moreover, some optical glass devices are not laser absorptive for both substrates and residual polishing particles, and have super-smooth substrate that has strong hydrophobic characterization. Furthermore, making a continuous and uniform liquid film of a few micrometers thick by steam condensation technique [12–14] is difficult. Therefore, the techniques of both steam laser cleaning and dry laser cleaning are not suitable for cleaning these types of optical glass surfaces.

This paper explores an analysis for cleaning poor laser-absorptive contaminated colloidal dioxide particles from poor absorptive and super-smooth optical glass substrate using a Nd:YAG laser having 1064 nm infrared (IR). The use of such a Nd:YAG laser to clean the contaminated colloidal dioxide particles requires new ideas to overcome the problem of poor absorptivity of both adhering dioxide particles and optical glass substrate, and also the problem of hardly condensing an aqueous thin film on the super-smooth substrate surface. A layer of volatile black paint film of a few micrometers thick was thus used to cover the contaminated particles on the substrate as shown in Fig. 1. Such a black paint layer aims at absorbing most fluence irradiating from a pulsed laser and thus creating explosive evaporation to thrust up the adhering particles without any remnant on the substrate surface. Furthermore, any residual contaminants, due to (i) the sputtering of re-condensation of vaporized paint vapor onto a specimen and (ii) re-descending of thrust-particles as a result of (i), can be further removed by either rinsing in distilled water or pressurized air blowing. Generally, nanosecond pulse lasers normally generate laser beam in ultra-violet (UV) band whilst millisecond pulse lasers usually emit IR beam. Although optical glass substrates have poor absorptivity to both UV and IR beams, they have relatively poorer absorptivity to IR. As successful cleaning implies that the surface integrity of a cleaned substrate should be properly maintained, the use of millisecond pulse lasers can minimize the absorption of laser fluence into the substrate and consequently alleviate any possible thermal effect to the surface of the optical glass substrate. Since the cleaning principle is to thrust the adhering SiO_2 and polished optical glass particles from the substrate surface by vaporizing the covering black paint film, the other advantages of using the millisecond pulse lasers, rather than the nanosecond pulse lasers [7–14], are: (i) lower energy density in avoiding possible surface damage of a substrate as the black paint film in irradiation spot is being completely evaporated; (ii) increasing cleaning efficiency due to larger irradiating spot; and (iii) the shape pattern of irradiating spot can be suitably adjusted and changed from circular to rectangular so as to control effectively the cleaning uniformity in a cleaning path.

Results of some preliminary experiments showed the workability of such approach was reasonably acceptable. However, the fact that the physical properties differ from the type of adhering particles and/or the black paint film to another type, from one thickness to another thickness of the painted film, leads to difficulty in the setting of the laser for proper removal of the particles and the assisting black paint film. To facilitate the effective performance of laser cleaning, preliminarily quantitative theory for the black paint film assisting laser cleaning should thus be produced. Due to the complex mechanisms involving with the evaporating paint film and with the removal of the colloidal silicon from the super-smooth glass surface, exact formulation of the laser cleaning seems impossible. An approximate upper and lower bound analysis to predict the maximum and minimum energy required for cleaning off the colloidal particles is thus proposed in this paper. The lower bound analysis predicts the laser fluence for overcoming the overall inertia and contact force of an adhering particle with the surface of substrate. The upper bound analysis predicts what amount of the required laser fluence is likely to damage the surface of substrate [16]. Scanning electron microscope (SEM) micrography of samples cleaned with laser fluence setting somewhere between the two bounds of the predicted limits gave good cleaning conditions on the surface. Experimental results showed that the adequate fluence setting in achieving good removal should be in the bound of approximately 10–20% below the upper threshold.

2. Theoretical model

The three modes of mechanisms in removing contaminant particles in a volatile solid film by a laser (Fig. 2) normally are: (a) lifting mode that occurs when the normal component F_p of a working force surpasses the inertia and overall contact force of particle with surface of substrate; (b) sliding mode that occurs when the tangential component

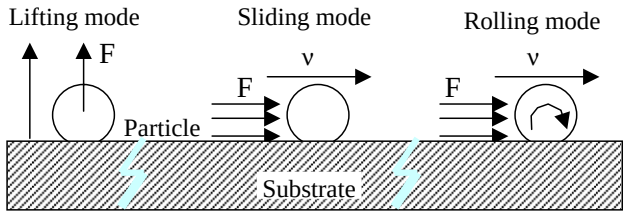

Fig. 2. Three mechanisms in laser removal of particles from a substrate.

F_s of a working force surpasses the static friction force on the particle; (c) rolling mode that occurs when the overall torque about a point contact is equal to zero (assuming that the force component to create such torque is force F_r). Although the actual mechanisms may be the combination of these three modes, exact analysis to proportionate the contribution of each mode is almost impossible. Since laser cleaning is mainly to burn off or to lift up the contaminant particles from the substrate surface, the components of the removing force contributing to the sliding mode and rolling mode in the laser cleaning are much less than the lifting mode [17]. Therefore, the minimum removal force F_L produced by the cleaning laser should be equal to and/or greater than the normal components of the lifting force F_p, i.e. $F_L \geqslant F_p$. In view of a cleaned substrate surface should preserve its integrity, also excessive laser fluence likely to damage the surface of a substrate, the upper bound of the incident laser fluence needs to be limited to that below the possible softening of the interfacial surface of a substrate.

2.1. Lower threshold of the laser beam force

Since the melting temperature of colloidal particles adhering on substrate surface is much higher than the volatile paint film, the intensive fluence of laser beam will vaporize the paint immerging the particles so rapidly that it would reasonably not create any adverse effect on the up-lifting of the particles (Fig. 1(b)). When a particle with mass m is lifted up to overcome (i) the gravitational acceleration g and (ii) the normal adhesion F_T between the particle and the super-smooth substrate surface, the particle removal force F_p can thus be approximated as $F_p > F_T + mg$. Subsequently, the lowest threshold of the force F_L generated by laser beam is thus expressed as

$$F_L = F_p > F_T + mg. \quad (1)$$

F_T in Eq. (1) can be used as a basis for setting laser fluence for removing contaminant colloidal silicon dioxide particles from the super-smooth optical substrate. Its analysis thus played an important role in saving the cost and time for the laser cleaning experiments.

2.1.1. Total inter-adhesion force

Adhesion forces between colloid and solid surface have been investigated both theoretically and experimentally as described in literature [18,19]. By simplifying the shape of colloidal particles as spherical, the total adhesion force between a particle and super-smooth substrate surface is thus composed of: (i) Van der Waals force (F_v), (ii) electrostatic attraction force (F_d) and (iii) capillary force (F_c). Instead of expressing F_T as a vectorial summation of the three captioned force components, its maximum value is taken as the three forces orientating in a same direction as

$$F_T = F_v + F_d + F_c. \quad (2)$$

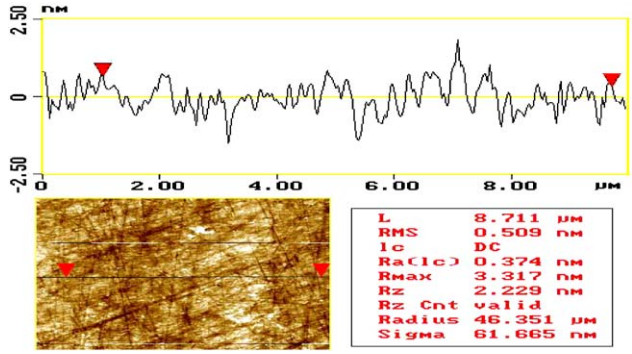

Fig. 3. SPM profile of a super-smooth surface.

2.1.1.1. Van der Waals force. According to Derjaguin–Mullur–Toporov (DMT) [19], the Van der Waals attraction F_v between a micron rigid particle with equivalent diameter d and a clean flat surface can be expressed as: $F_v = hd/(16\pi z^2)$, where h is a material-dependent Liftshitz–Van der Waals constant, and z is the atomic separation between the particle and the actual flat surface. Although roughness on physical surfaces inevitably affects the magnitude of F_v [20], the measured roughness of super-smooth substrate was only 0.374 nm (Fig. 3), which has negligible effect on the value of van der Waals interaction and thus can be assumed completely flat. Furthermore, much harder of optical substrate than the particles of colloidal silicon dioxide allows the assumption of the attraction to be only sufficient to deform the colliodal silicon dioxide. As a result, the DMT model [19] describing the attractions between the particle and substrate is not applicable. In view of the fact that the mutual attraction between the colloidal silicon dioxide particles and the rigidly super-smooth optical glass would result in compressive interactions at the central contact zone and tensile interactions around its outer surrounding, the Johnson–Kendall–Roberts (JKR) model [21] of adhesion force is thus used, which is

$$F_v = 3(\gamma_1 + \gamma_2 - \gamma_{12})\pi R/2, \quad (3)$$

where γ_1 and γ_2 are the surface tension of particle and substrate, respectively, γ_{12} is their interfacial surface tension, and normally $(\gamma_1 + \gamma_2 - \gamma_{12}) = 2\sqrt{\gamma_1\gamma_2}$.

2.1.1.2. Electrostatic attraction. A colloidal particle acquires charges when its surface is exposed to a liquid. Due

to the weak alkalesence of silicon dioxide particles within a paint film of colloidal suspension, the surfaces of both particles and super-smooth substrate are charged electrostatically with opposite sign. The electrostatical charging at the interface between the colloidal film of silicon dioxide and the substrate is normally termed as "electrical double layer". The force F_d in the electrical double layer thus plays an important role in adhering the micro-particles onto the substrate surface. Let the colloidal particle with radius R be spherical and the contact potential of its contacting surface, z away from the super-smooth substrate, be $\Delta\psi$, the attraction F_d of the double layer charge is thus expressed [21,22] as

$$F_d = \pi\varepsilon_0(R/z)(\Delta\psi)^2, \tag{4}$$

where ε_0 is the permittivity of free space, and $\Delta\psi$ is generally taken in range of 0.0–0.5 V.

2.1.1.3. Capillary force. The assumed spherical silicon dioxide with radius R possibly forms a convegent and divergent channel with the substrate surface (Fig. 2), which creates a capillary action to drag in the applied black paint film that melts under laser irradiation. The wetted surface of these Si dioxide particles by the residual melting film with surface tension γ_3 produces a capillary force F_c approximated as

$$F_c = 4\pi\gamma_3 R. \tag{5}$$

2.1.1.4. Total adhesion force F_T. Substituting Eqs. (3)–(5) into Eq. (2) allows F_T to be written as

$$F_T = (3/2)(\gamma_1 + \gamma_2 - \gamma_{12})\pi R + \pi\varepsilon_0(R/z)(\Delta\psi)^2 + 4\pi\gamma_3 R. \tag{6}$$

Eq. (6) establishes the lower threshold of the lifting force F_p to overcome the adhesion force F_T and the gravitational force mg of a contaminant particle (see Eq. (1)). For removing the contaminants using a laser system, the laser fluence must be sufficient to generate this lowest limit of F_p. Substituting Eq. (6) into Eq. (1) gives the lower threshold of a laser cleaning force F_p.

2.2. Upper threshold of laser beam force

The proposed laser cleaning method (Fig. 1) involves with the application of a thin film of h_o thick black paint, covering the silicon dioxide particles adhering on a super-smooth optical substrate. The cleaning action is accomplished by the incidence of fluence sufficiently high to evaporate the black paint that generates pressure thrust to lift the adhering particles away from the surface of the substrate. As a laser beam with focusing diameter D is irradiating on the pasted paint film, the expansion of the paint on top of adhering particles may have residual pressure to reduce the lifting effect of the particle by the subsequent evaporation of the paint below. Modeling in this paper assumes the laser intensity being sufficiently high to evacuate rapidly the preceding evaporated layer of paint so that the residual effect is negligible. As a result, the explosive shock wave generated by evaporation of the paint from the bottom semi-spherical half surface of a contaminant pushes the contaminant upwardly away from the super-smooth surface [23,24]. Although high incident laser fluence q always creates high explosive evaporation, too high the value of q may possibly burn the substrate surface in the cleaning operation, which subsequently degrades the functionality of the substrate. Preserving surface integrity of a substrate (Section 1) is therefore one of the prime important issues for determining the success of a cleaning method. The upper threshold of laser fluence in laser cleaning thus limits the minimal thermal energy just at a verge to skin-melt slightly the substrate surface. As the modeling is only an approximation, it therefore assumes that the applied black paint film and the contaminant silicon dioxide particles structurally form among themselves as a monolithic layer on the substrate layer, thus creating a two-layer system with perfect thermal contact interface. The fast evaporation rate of the paint under laser irradiation means that (i) the effect of latent heat of paint on the temperature and fluence, and (ii) the heat transfer to the surrounding of a focusing area $A_f(=\pi D^2/4$, see Fig. 1) are negligible. Therefore, the laser fluence distribution over A_f is assumed uniform [16] and the conductive heat dispersion in the effective thermal column $A_f h_o$ is one dimensional from top to bottom of the black paint film. Moreover, the absorbed laser fluence by the irradiated surface in a thermal column $A_f h_o$ is assumed approximately equal to qA_f, and the evaporating vapor of the black paint is assumed obeying the law of ideal gas. As only the upper threshold of fluence energy is interested in the analysis, it is further assumed that the laser fluence in a thermal column is effectively constrained within the column itself.

2.2.1. Heat transfer analysis in laser cleaning

Assume that there is not any plasma formation at and on the surface being irradiated by the incident laser fluence, the governing heat conductive equation and the relevant boundary conditions for the monolithic layer can be written as [20]

$$\frac{\partial T_f(x,t)}{\partial t} = \alpha_f \frac{\partial^2 T_f(x,t)}{\partial x^2}, \quad t > 0,\ 0 \leqslant x \leqslant h_0 \tag{7}$$

and for the substrate as

$$\frac{\partial T_s(z,t)}{\partial t} = \alpha_s \frac{\partial^2 T_s(z,t)}{\partial z^2}, \quad t > t_s,\ 0 \leqslant z \leqslant \infty,\ z = (x - h_0), \tag{8}$$

where T is the excess temperature compared with the ambient temperature T_a, at an interested location x away from the paint surface, $\alpha = \kappa/\rho C_p$ is the thermal diffusivity in terms of the thermal conductivity κ and the heat capacity per unit volume ρC_p, t_s is the time taken for the excess temperature T, at the interface between paint film and substrate, to change from zero, α_f and α_s are, respectively, the thermal diffusivity of the film and the substrate, κ_f and κ_s

are, respectively, the thermal conductivity of the film and the substrate, $\rho_1 C_{p1}$ and $\rho_2 C_{p2}$ are, respectively, the heat capacity per unit volume of the film and the substrate. Further initial and boundary conditions of temperature and heat transfer for both monolithic layer and substrate layer are

$$T_f(x,0)=0;\ T_s(z,0)=0;$$

$$-\kappa_f \left.\frac{\partial T_f}{\partial x}\right|_{x=0} = qA_f;\ T_f(h_0,t)=T_s(0,t);$$

$$-\kappa_f \left.\frac{\partial T_f(x,t)}{\partial x}\right|_{x=h_0} = -\kappa_s \left.\frac{\partial T_s(z,t)}{\partial z}\right|_{z=0};$$

$$T_s(\infty,t)=0. \tag{9}$$

Use of Laplace transforms to transfer the time variables in both Eqs. (7) and (8) gives

$$\frac{\partial^2 \bar{T}_f(x,s)}{\partial x^2} - \frac{s}{\alpha_f}\bar{T}_f(x,s)=0,$$

$$\frac{\partial^2 \bar{T}_s(z,s)}{\partial z^2} - \frac{s}{\alpha_s}\bar{T}_s(z,s)=0, \tag{10}$$

where $\bar{T}_f(x,s)$ and $\bar{T}_s(z,s)$ are, respectively, the Laplace transform of T in the region of film and substrate. Subsequently, the Laplace transform of the boundary conditions in Eq. (9) can be written as follows:

$$-\kappa_f \left.\frac{\partial \bar{T}_f(x,s)}{\partial x}\right|_{x=0} = \frac{qA_f}{s};\ \bar{T}_f(h_0,s)=\bar{T}_s(0,s);$$

$$-\kappa_f \left.\frac{\partial \bar{T}_f(x,s)}{\partial x}\right|_{x=h_0} = -\kappa_s \left.\frac{\partial \bar{T}_s(z,s)}{\partial z}\right|_{z=0};$$

$$\bar{T}_s(\infty,s)=0. \tag{11}$$

The solutions of Eq. (10) can be written in the form

$$\bar{T}_f(x,s)=\sum_{n=0}^{\infty}\frac{qA_f}{\kappa_f s\sqrt{s/\alpha_f}} \times\left\{B^{n+1}\exp\left(-\sqrt{s/\alpha_f}[2(n+1)h_0-x]\right) +B^n\exp\left(-\sqrt{s/\alpha_f}[2nh_0+x]\right)\right\},$$

$$\bar{T}_s(z,s)=\frac{2qA_f}{\kappa_f s\sqrt{s/\alpha_f}(1+\xi)}\sum_{n=0}^{\infty}B^n\exp\left(-\sqrt{s/\alpha_f}\left[(1+2n)h_0 +z\sqrt{\alpha_f/\alpha_s}\right]\right), \tag{12}$$

where $\xi=(\kappa_s/\kappa_f)\sqrt{s/\alpha_s}/\sqrt{s/\alpha_f}=\kappa_s/\kappa_f\sqrt{\alpha_f}/\sqrt{\alpha_s}$, and $B=(1-\xi)/(1+\xi)$. Let $F(s)=1/(s\sqrt{s/\alpha_f})\exp(-\sqrt{s/\alpha_f}x)$ and the inverse transform of $F(s)$ be as

$$L^{-1}\{F(s)\}=2\sqrt{\alpha_f t/\pi}\exp\left(\frac{-x^2}{4\alpha_f t}\right) -x\mathrm{erfc}\frac{x}{\sqrt{4\alpha_f t}},\quad x>0,\ \alpha_f>0 \tag{13}$$

in which erfc is a complementary error function. Using the inverse Laplace transform, $\bar{T}_f(x,s)$ and $\bar{T}_s(z,s)$ in Eq. (12) can be, respectively, transformed to

$$T_f(x,t)=\sum_{n=0}^{\infty}\frac{qA_f}{\kappa_f}B^{n+1}\left(\sqrt{4\alpha_f t/\pi} \times\exp\left\{-\frac{[2h_0(1+n)-x]^2}{4\alpha_f t}\right\} -[2h_0(1+n)-x]\mathrm{erfc}\frac{2h_0(1+n)-x}{\sqrt{4\alpha_f t}}\right) +\sum_{n=0}^{\infty}\frac{qA_f}{\kappa_f}B^n\left\{\sqrt{4\alpha_f t/\pi}\exp\left[-\frac{(2nh_0+x)^2}{4\alpha_f t}\right] -(2h_0 n+x)\mathrm{erfc}\frac{2h_0 n-x}{\sqrt{4\alpha_f t}}\right\}$$

and

$$T_s(z,t)=\sum_{n=0}^{\infty}\frac{2qA_f}{\kappa_f}\frac{B^n}{(1+\varepsilon)}\left(\sqrt{4\alpha_f t/\pi} \times\exp\left\{-\frac{[z\sqrt{\alpha_f/\alpha_s}+(1+2n)h_0]^2}{4\alpha_f t}\right\} -[z\sqrt{\alpha_f/\alpha_s}+h_0(1+2n)] \times\mathrm{erfc}\left\{\frac{[z\sqrt{\alpha_f/\alpha_s}+(1+2n)h_0]}{\sqrt{4\alpha_f t}}\right\}\right). \tag{14}$$

The temperature on the surface of the applied paint film can subsequently be obtained by the substitution of $x=0$ into the first expression of Eq. (14) as

$$T_f(0,t)=\sum_{n=0}^{\infty}\frac{qA_f}{\kappa_f}B^{n+1}\left(\sqrt{4\alpha_f t/\pi}\times\exp\left\{-\frac{[2h_0(1+n)]^2}{4\alpha_f t}\right\} -[2h_0(1+n)]\times\mathrm{erfc}\frac{2h_0(1+n)}{\sqrt{4\alpha_f t}}\right) +\sum_{n=0}^{\infty}\frac{qA_f}{\kappa_f}B^n\left\{\sqrt{4\alpha_f t/\pi}\exp\left[-\frac{(2nh_0)^2}{4\alpha_f t}\right] -2nh_0\times\mathrm{erfc}\frac{2h_0 n}{\sqrt{4\alpha_f t}}\right\},$$

$$T_s(0,t)=\sum_{n=0}^{\infty}\frac{2qA_f}{\kappa_f}\frac{B^n}{(1+\varepsilon)}\left(\sqrt{4\alpha_f t/\pi} \times\exp\left\{-\frac{[(1+2n)h_0]^2}{4\alpha_f t}\right\}-h_0(1+2n) \times\mathrm{erfc}\left\{\frac{[z\sqrt{\alpha_f/\alpha_s}+(1+2n)h_0]}{\sqrt{4\alpha_f t}}\right\}\right). \tag{15}$$

Eqs. (14) and (15) provide a mean for proper selection of the laser fluence for an anticipated cleaning. The time t taken to accomplish the upper temperature limit $T_f(0,t)$ that softens the surface of substrate material at the bottom surface of the applied paint film is firstly computed using Eq. (15). Its value is then substituted into the second and first expressions of Eq. (14) for estimating the temperature profile within the film and the surface temperature of the film, respectively. By doing so, the upper threshold of the laser fluence can be determined after the justification of whether force generation matching that calculated in Section 2.2.2 below.

2.2.2. Laser cleaning force

The strong shock wave generated by explosive vaporization of the applied paint film under irradiation of high laser fluence [23,24] pushes the micro-contaminants upwardly from the optical substrate surface. Such pushing force must be much larger than the adhesion force F_T as described by Eq. (1). Assuming that the distribution of applying pressure over the irradiated area A_f is uniform and the thermodynamic of the vaporized paint can be treated as ideal gas, the explosive vapor pressure P_v at a vaporization temperature T_s can thus be related as [25,26]

$$P_v = P_b \exp\left[\frac{\Delta H_v}{M_0}\left(\frac{1}{T_b} - \frac{1}{T_s}\right)\right], \tag{16}$$

where ΔH_v is the enthalpy of vaporized paint at boiling temperature T_b; M_0 is the universal gas constant; P_b is the saturated vapor pressure of the melted paint at a known boiling temperature T_b. P_b should be sufficiently large to complete the vaporization of the black paint in an effective thermal column $A_f h_o$, and is thus expressed as

$$P_b = P_0 + \rho_1 g h_0/2 + 4\gamma_3/D, \tag{17}$$

in which $P_0 = 1.01325 \times 10^5$ N/m^2 is the ambient atmospheric pressure, $\rho_1 g h_0$ is the static pressure of the melting black paint that has density ρ_1, g is the acceleration of gravity, γ_3 is the surface tension of the melting black paint, and D is the laser beam diameter.

Successful removal of a contaminant from the surface of a super-smooth substrate by the vaporizing black paint film requires sufficiently large laser cleaning force F_L to overcome the resultant of the viscous resistance of the vaporizing black paint and the atmospheric pressure acting on the film. The laser cleaning force F_L can thus be related to both P_v and P_b as

$$F_L = \pi R^2 (P_v - 6\pi R\gamma_3 V - P_b), \tag{18}$$

where R is the radius of the contaminant particle; γ_3 is the surface tension of the melted paint film; $V \approx 10^2$–10^3 m/s is the moving velocity of contaminant. Eq. (18) provides the theoretical upper threshold of the laser cleaning force F_L for lifting the contaminant particle from the adhered surface of a substrate.

3. Numerical predictions

Successful laser cleaning requires a sufficiently large laser irradiating fluence to vaporize the black paint film producing a lifting force larger than Eq. (1) and smaller than Eq. (18). Eq. (18) limits the laser fluence to prevent the glass substrate surface from damage. Although the higher laser fluence certainly gives better cleaning effect, it has higher probability in degrading the servicing quality of the substrate. Numerical prediction to determine the laser cleaning threshold and the substrate damage threshold governs the proper selection of laser fluence. Predictions using analysis in Section 2 and the parameters in Table 1 were performed and presented in Figs. 4–8.

3.1. Selection of laser fluence

At a specific pulse of a pulse laser, the achievable surface temperature T_s of the black paint film interfacing with the substrate increases linearly with the laser irradiating fluence (Fig. 4). The rate of increment increases with pulse duration. At the respectively selected pulse duration of 1, 5, 10, 15, and 20 ms, the corresponding laser fluence to initiate the vaporization of the applied paint film surface is 14×10^6 (i.e. 14 J/mm^2), 8.13×10^6, 6.25×10^6, 5.13×10^6, and 4.87×10^6 J/m^2. Whilst the corresponding estimated value for commencing the melting of substrate is approximately at 45.8×10^6 (i.e. 45.8 J/mm^2), 25.7×10^6, 20.1×10^6, 15.6×10^6, and 14.8×10^6 J/m^2. The effective laser fluence selected should therefore lie between the individual predicted threshold pairs.

3.2. Threshold of vaporization pressure and laser fluence

Fig. 5 shows the relationship between the surface temperature and the vaporization pressure of the film. When the film vaporization pressure reaches the value of 2.75×10^6 N/m^2, the temperature of the film is approximately equal to the melting point of the optical substrate. This indicated that the vaporization pressure of the film should always be kept below 2.75×10^6 N/m^2, otherwise damage of the substrate surface occurs. Fig. 6 shows the temperature distribution across the film thickness when the irradiating laser pulse duration is at 5, 10, 15, and 20 ms, respectively. It illustrates that the paint film surface is below its vaporization temperature of 1275°K [27] when laser fluence q is equal to 5×10^6 J/m^2, implying that the laser fluence obviously can never remove any contaminated colloidal particle from an optical substrate. When the laser is operating at a fluence q of 10×10^6 J/m^2 with pulse durations beyond 15 ms, the removal of the contaminants may barely occur since the temperature in the paint film is just ranging between its boiling and evaporation points. When a laser with fluence q of 20×10^6 J/m^2 and pulse duration of either 15 or 20 ms is irradiating a paint film, the bottom temperature of the film

Table 1
Parameters used in numerical predictions

h_o (μm)	A_f	ΔH_{1v} (J/mol)	z (m)	ε_o (A^2 s^4/m^2 kg)	γ_1 (N/m)
3	0.82	34008	4×10^{-9}	8.85×10^{-12}	18×10^{-3}
ρ_1 (kg/m^3)	ρ_2 (kg/m^3)	ρ_p (kg/m^3)	κ_s (W/m K)	C_{p1} (J/kg K)	γ_3 (N/m)
1380	2650	2560	1.114	117	47.8×10^{-3}
T_{ms} (K)	T_m (K)	T_b (K)	κ_f (W/m K)	C_{p2} (J/kg K)	γ_2 (N/m)
2502.2	590.2	820	0.15	720	10.1×10^{-3}

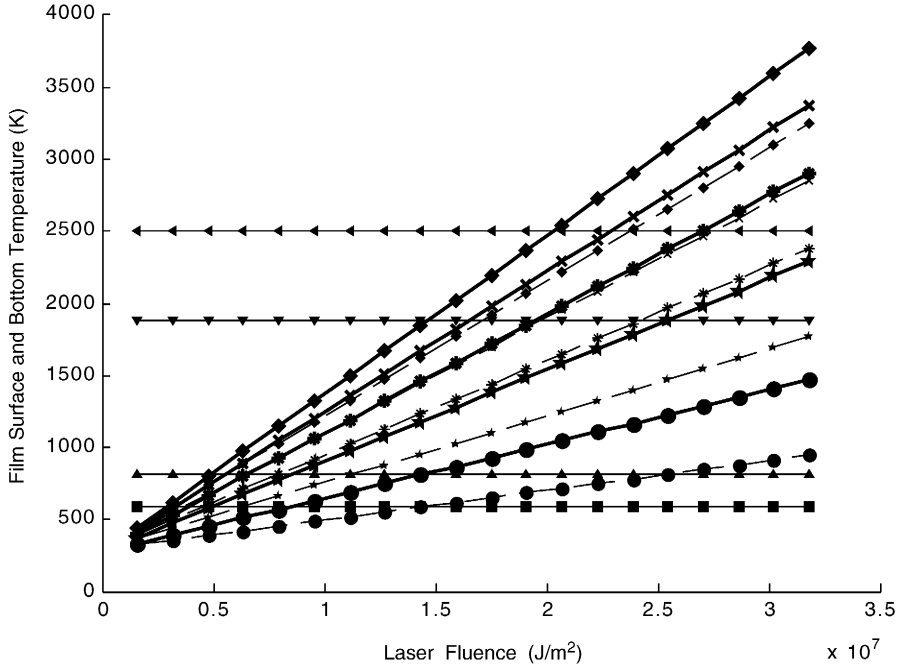

Fig. 4. Predicted surface and bottom temperature of the film at different levels of laser energy fluence. Pulse duration (t_s): ● 1 ms; ★5 ms; ∗10 ms; ×15 ms; ♦ 20 ms. Temperature of: ■ melting of film; ▲ boiling of film; ▼ softening of substrate; ◀ melting of substrate. Temperature for: —surface of the film; – –bottom of the film.

is thus exceeding the softening temperature 1883.4°K of the optical substrate. Meanwhile when q is at 15×10^6 J/m^2 and pulse duration is 10 ms, the bottom temperature of the paint film is closer to the substrate softening temperature that is likely to vaporize the film and yet to keep the integrity of the surface of the substrate.

3.3. Optimal laser fluence for laser cleaning

Numerical prediction provides information for better selection of the laser fluence for laser cleaning operations. However, the range is so wide (Sections 3.1 and 3.2) that it requires further narrowing down in order to facilitate the effective cleaning operation. When the vaporizing pressure of the paint film is sufficiently high, the vaporized paint tends to thrust up the adhering contaminants rapidly from the substrate surface. Fig. 7 illustrates the individual characteristics and the contribution of van der Waals force, electrostatic force and capillary force to the overall adhesion of a particle

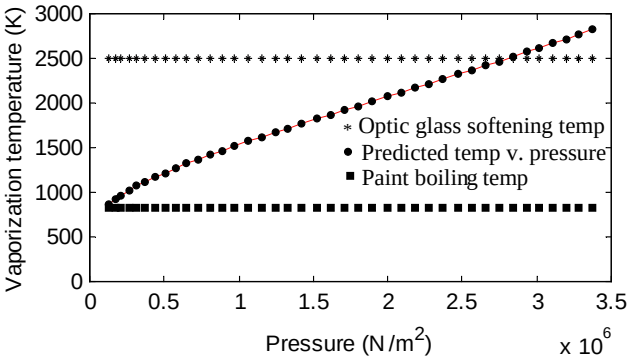

Fig. 5. Relationship between film vaporization temperature and pressure.

having radius R. It indicates that the contribution of Van der Waals force is dominantly large whilst the capillary force is almost insignificantly small. For a polishing colloidal silicon dioxide with size of 0.2 μm adhering onto a super-smooth glass substrate, its overall adherence force was calculated as

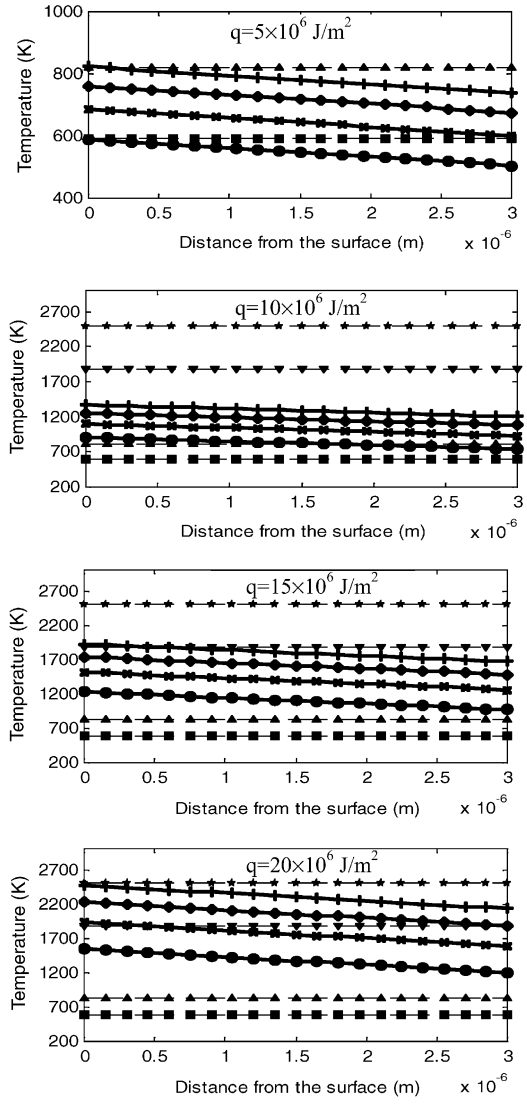

Fig. 6. Temperature distribution in film thickness for film irradiated at different levels of laser fluences. Temperature for - Pulse duration: • $t_s = 5$ ms; × $t_s = 10$ ms; ♦ $t_s = 15$ ms; + $t_s = 20$ ms. Paint film: ■ Melting; ▲ Boiling; Substrate: ▼ Softening of substrate; ∗ Melting of substrate.

0.399×10^{-6} N, that is 3.668×10^9 times of the value for the relative gravity of the particle. Any practical cleaning method is difficult to achieve so huge an acceleration except an efficient laser cleaning technique. The cleaning force produced by the vaporization pressure of the black paint film for removing a particle of radius R can easily be evaluated from Fig. 8. The relationship of vaporization pressure and the particle removal force as shown in Fig. 8 illustrates that the cleaning force is smaller than the adhesion force when the radius of the particles is 0.1 μm, thus implying that the contaminant particle can never be removed under such circumstance. As the particle radius increases to 0.2 μm, the laser cleaning force becomes larger than the adhesion force of a particle when the vaporization pressure is beyond the

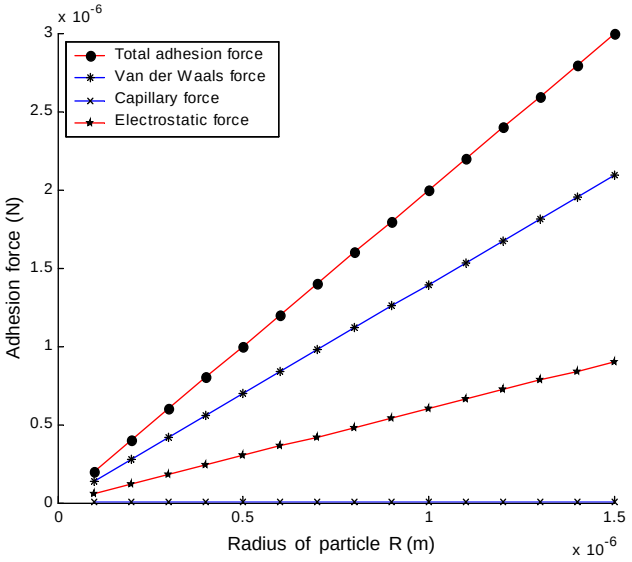

Fig. 7. Relationship between particle radius and different adhesion force.

value of 1.5×10^6 N/m^2 and the laser fluence is ranging from 14.35×10^6 to 20×10^6 J/m^2 (Figs. 4–6). From Figs. 5 and 8, the lowest laser fluence likely to start the movement of the contaminant particle with radius of 0.3 μm (Fig. 4) can be evaluated as 10.6×10^6 J/m^2. Generally, the larger the particle radius is the wider the selection range of laser fluence is for removing the contaminant particle. The numerical investigation undertaken in this study limits the size of polishing colloidal silicon dioxide from 400 to 600 nm, also the selection of laser fluence for removing the contaminant particles at and beyond 0.4 μm in a 3 μm thick black paint film ranges from 14.35×10^6 to 20×10^6 J/m^2.

4. Experimental validation

Effective laser cleaning technique should completely remove the contaminated particles from a substrate surface and yet retain the surface free from damage. Since the cleaning objects are poor absorption to IR and UV laser, and super-smooth optical substrate surface has strong hydrophobic feature, black paint film is thus used to cover the contaminant particles on top of the substrate surface to form a colloidal film for assisting laser cleaning. Experimental validations of the proposed method incorporating the predictions in Section 3 were thus conducted.

4.1. Experimental setup

A KLS 522 multi-mode Nd:YAG laser made by Switzerland LASAG Corporation was used in the experimental system as shown in Fig. 9. The Nd:YAG laser has a wavelength of 1064 nm, pulse width in the range of 0.05–20 ms with a maximum pulse repetition rate of 1000 Hz, a maximum peak pulse power of 6 kW, and average pulse energy of

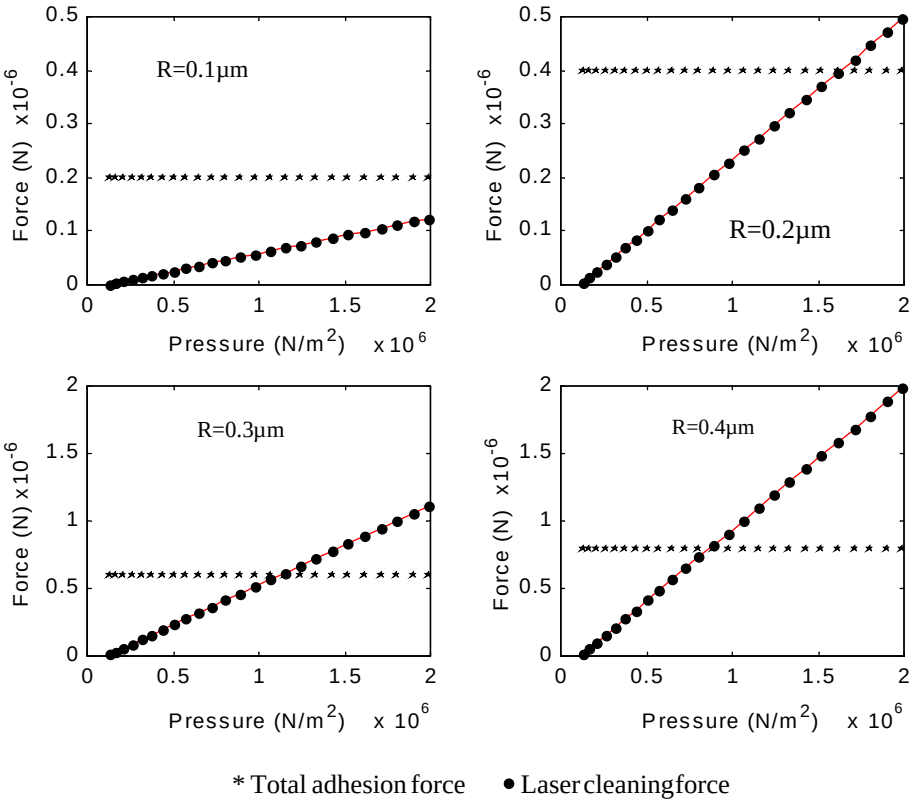

Fig. 8. Relationship between laser cleaning force and vaporization pressure.

250 W and maximum pulse energy of 50 J. The laser would be adjusted to give focal spots with diameter 0.2, 0.5, 1, and 1.5 mm, respectively, by suitably installing lens with focal length corresponding to 50, 100, 125, and 150 mm. For the experimental investigations below, the laser was set to give a focal spot with diameter 0.5 mm and the pulse duration was set at 15 ms.

4.2. Sample preparation

The original surface of specimens used in this experimental study was taken after chemical machining process (CMP) and all the large and loose particles prior to laser cleaning were removed by ultrasonic cleaning method. The micro-contaminants on optical substrates in the experiments were composed of the suspension of polishing colloidal powders of silicon dioxide and particles of the polished substrate itself, with sizes likely to be smaller than 600 nm. SEM was used to take photographs of the contaminant particles on a post-CMP surface of optical glass substrate (Fig. 10). Thin film of black paint, which was volatile under the intensive irradiation of laser fluence, was sprayed on the surfaces of specimens in a container, with the spraying speed being suitably controlled to give spray thickness of 0.1 μm/min. SEM morphology of sprayed film on an optical substrate surface was shown in Fig. 11.

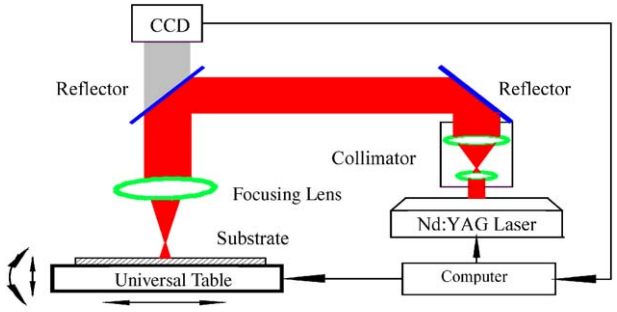

Fig. 9. Schematic diagram of the laser cleaning system.

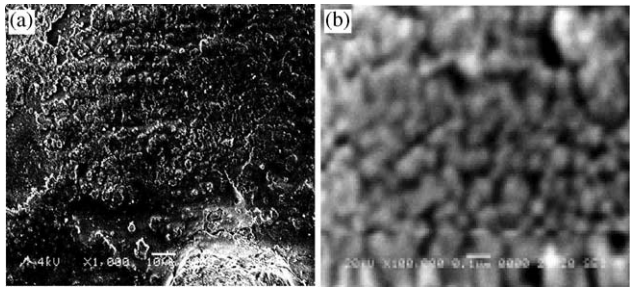

Fig. 10. Colloidal silica on the surface of Post-CMP K8 substrate.

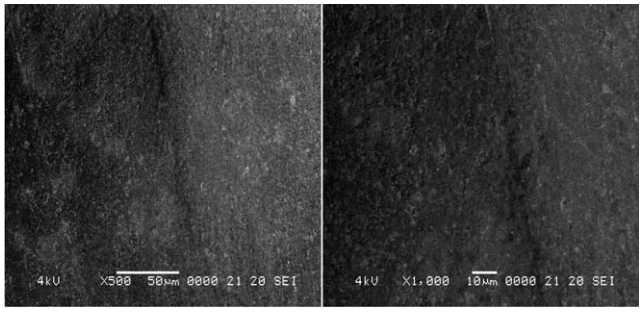

Fig. 11. Topography of a thin film coated on a post-CMP substrate surface.

4.3. Laser cleaning tests

Specimen was mounted on a specially designed and computer-controlled universal inspecting table having six free degree of motion. The incident laser-eradicated colloidal film at a preset place on the specimen at different angles by controlling the linear and rotary motion of the universal table. Cleaning path and profile were normally dependent on the thickness and vaporization point of the black paint sprayed on substrate surface. Change in fluence irradiating on substrate surface was achieved by adjusting the beam diameter, pulse duration, and pulse frequency in computer software. Correct diameter and size adjustment of laser beam was identified by a burn pattern that allowed estimating the average fluence of individual settings. The nature of multimode and non-Gaussian beam profile of the laser system gave approximately uniform intensity so that the fluence in the experiments was therefore an average value of the beam. The energy of laser was automatically detected by an energy-measuring instrument and displayed on a computer monitor. A charge-coupled device (CCD) with 5–2000 times of magnification was used to in situ visualize the cleaning process whilst SEM was used to analyze the laser-cleaned specimens. Furthermore, a particle recognition system was used to analyze on-line the image captured by both CCD optical microscope and the off-line image of SEM. Tests were performed firstly by setting the required laser fluence, focal spot diameter, and pulse duration of the Nd:YAG laser, then starting the laser to spot-irradiate the paint film accordingly.

4.4. Results and validation of the cleaning laser fluence

Experiments were performed to validate the predictions of laser fluence required in removing the contaminant particles from super-smooth substrate surface. Surface morphology (Fig. 12) of the irradiated zone of black paint film with 300 nm thickness under various fluence of a single laser validated the change of cleaning efficiencies of the substrate surface with incident laser fluence. At low fluence of 5×10^6 J/m^2 that was below the predicted lower threshold to remove contaminants and above the fluence to commence the melting of the paint film (Fig. 4), surface

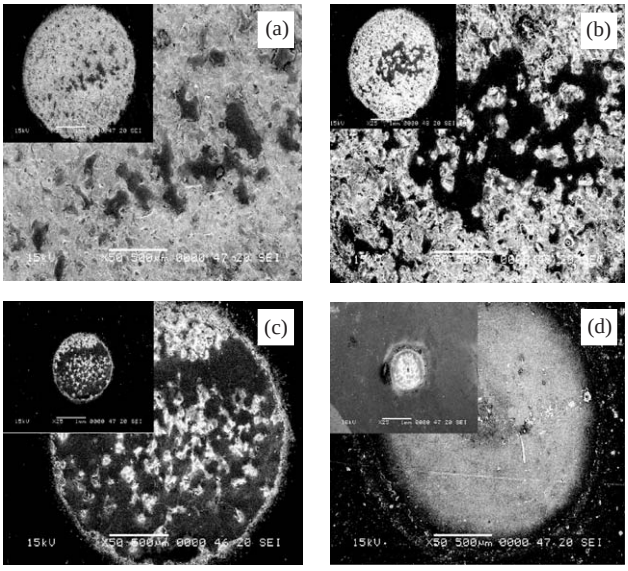

Fig. 12. Surface morphology of laser cleaning, 3 μm thickness film on the substrate surface: (a) $q = 5 \times 10^6$ J/m^2; (b) $q = 9.34 \times 10^6$ J/m^2; (c) $q = 11.21 \times 10^6$ J/m^2; (d) $q = 15.2 \times 10^6$ J/m^2.

morphology of the laser irradiated zone (Fig. 12(a)) showed that the super-smooth substrate surface was still vividly covered with a layer of remelting paint compound with relatively stronger level of remelting in the center than that around its surrounding. When the laser fluence was increased to 9.34×10^6 J/m^2, surface morphology of the laser-irradiated zone (Fig. 12(b)) revealed the occurrence of a relatively larger vaporized region on film that unveiled some regions of the bare super-smooth surface, showing the inefficient removal of the film. Although the surface morphology showed sight of the nonuniformity of the laser energy distribution that undisputedly affects the results of cleaning experiments, the exploration of the vaporized surface of the irradiated film deduced that the hypothesis of approximate uniform energy across the focusing spot was permissible. By further increasing the laser fluence to 11.21×10^6 J/m^2, SEM morphology (Fig. 12(c)) showed the exposure of substantially larger regions of substrate surface with some film remains scattering over the irradiated zone. The morphology suggested the film evaporation (Fig. 12(c)) becomes the major cleaning mechanism under the operational conditions, and higher cleaning efficiency has been acquired when compared with that shown in Fig. 12(b). At fluence of about 15.2×10^6 J/m^2, surface morphology in Fig. 12(d) gave idea that the film and particles were almost completely eradicated under the irradiation of laser. The almost evenly distributed texture pixel on the cleaned surface implied the cleaning due to vaporization of film rectified the non-uniformly distributed fluence across the laser focal spot. However, the darker pixel in the middle of irradiated zone (Fig. 12(d)) was identified as trace of re-solidification of some melted substrate material affecting the reflection of light. This observation shredded light that

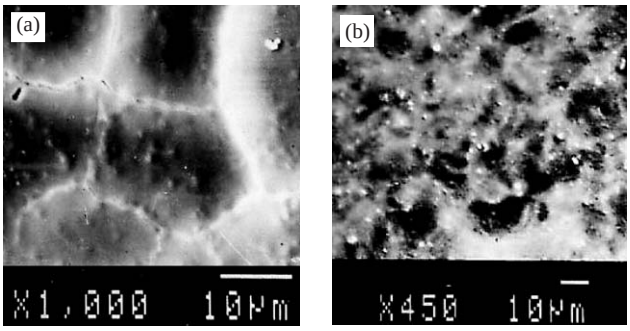

Fig. 13. Laser cleaning surface with defects under improper parameters: (a) $q = 18.8 \times 10^6$ J/m^2; (b) $q = 23.8 \times 10^6$ J/m^2.

the laser fluence of 15.2×10^6 J/m^2 was the critical value (i.e. the upper threshold—see Fig. 4 and Section 3.1) for complete removal of the particles from the substrate surface sprayed with black paint film of 3000 nm thick. When the laser fluence was set at 18.8×10^6 J/m^2, cracks on cleaned surface was observed (Fig. 13(a)) and seemed to propagate around the interphase of glass crystallite due to the heat-induced surface distensible fracture. When the laser fluence ascends to 23.8×10^6 J/m^2, the irradiated substrate surface (Fig. 13(b)) gave sight of evaporation of substrate material. The laser fluence corresponding to crack generation on an irradiated optical super-smooth surface would be called cleaning damage threshold. Results of these experiments were almost consistent with the prediction and indicated that the fluence for the effective cleaning should lie between 11.21×10^6 and 15.2×10^6 J/m^2, preferentially within 10–20% below the estimated upper threshold (see Fig. 4 and Section 3.1).

5. Conclusion

Implementing a layer of black paint film covering the contaminated particles on the substrate surmounted the difficulty of laser cleaning of poor laser absorptive silicon dioxide contaminants from super-smooth glass surface. An approach of limit analysis was proposed to provide data for selecting parameters for the laser cleaning process. Predictions of the limit analysis indicated the dependency of temperature and pressure on the operating laser fluence, which also governed the cleanliness and the cleaning efficiency of a laser cleaning system. Predicted data also gave the lower threshold of laser fluence to initiate the boiling of pain film at the interface of film and substrate, and the upper threshold of threshold that likely initiated the softening of the substrate surface. Experiments on cleaning micro-particles on K8 optical glass showed that the data predicted by the limit analysis were reasonably agreeable with the experimental results, also that the working laser fluence should be in the range of 80–90% of the predicted upper threshold value.

Acknowledgements

Most of the work described in this paper was supported by a Grant from the Research Grants Council of Hong Kong special administrative Region, China (Project No. 7001064 CityU). Some experimental data were derived from the support by a grant from the National Science Foundation of China (Project No. 59775075).

References

[1] Kuehn TH, Kittleson DB. Particle removal from semiconductor wafers. In: Fury MA, editor. The early days of CMP. Solid State Technol; May 1997.
[2] Hou RX. Present application of supersonic in cleaning optical parts. Opt Technol 1996;3:44–7.
[3] Hills MM. Carbon dioxide jet spray cleaning of molecular contaminants. J Vac Sci Technol A 1995;13(1):30–4.
[4] Christenson KK. Rinsing: a critical process in contamination removal. J Inst Environ Sci 1997;40(5):45–50.
[5] Winter DK. Large area plasma cleaning with microwave slot antenna plasma source. Surface Coating Technol 1997;93:134–41.
[6] Cumbo MJ. Slurry particle size evolution during the polishing of optical glass. Appl Opt 1995;34(19):3743–55.
[7] Britten JA. A moving-zone magangoni drying process for critical cleaning and wet processing. Solid State Technol 1997;40(10):143–7.
[8] Tam AC, et al. Laser-cleaning techniques for removal of surface particulates. J Appl Phys 1992;71(7):3515–23.
[9] Kelley JD, Hovis FE. A thermal detachment mechanism for particle removal from surfaces by pulse laser irradiation. Microelectron Eng 1993;20(1–2):159–70.
[10] Krusell WC, de Larios JM, Zhang J. Vacuum ultraviolet substrate cleaning and etching. Solid State Technol 1995;38(6):109–13.
[11] Lu YF, Zhang Y, Wan YH. Laser cleaning of silicon surface with deposition of different liquid films. Appl Surf Sci 1999;138–139:140–4.
[12] Yong-Feng Lu, Wen-Dong Song, Teck-Seng Low. Laser cleaning of micro-particles from a solid surface—theory and application. Mater Chem Phys 1998;54:181–5.
[13] Lu YF, Song WD, et al. A theoretical model for laser removal of particles from solid surfaces. Appl Phys A 1997;65:9–13.
[14] Lu YF, Song WD, Hong MH, Zheng YW, Chong TC. Laser surface cleaning and potential applications in disk drive industry. Tribol Int 2000;33:329–35.
[15] Tam AC, Park HK, Grigoropoulos CP. Laser cleaning of surface contaminants. Appl Surf Sci 1998;127–129:721–5.
[16] Akia Tsunemi, Koji Hagiwara, et al. Complete removal of paint from metal surface by ablation with a TEA CO_2 laser. Appl Phys A 1996;63:435–9.
[17] Wang HC. Effects of inceptive motion on particle detachment from surface. Aerosol Sci Technol 1990;13:386–93.
[18] Stainton C, Liang W, Kendall K. Formation and fraction of adhesive bonds between colloidal spheres. Eng Fracture Mech 1998;61:83–91.
[19] Pocius AV. Adhesion and adhesion technology. New York: Hanser Publishers; 1997.
[20] Mittal KL. Particles on surfaces. New York, Basel, Hong Kong, New York: Marcel Dekker; 1995.
[21] Rimai DS, Sharpe LH. Advances in particle adhesion. Orlando: Gordon and Breach Publishers; 1996.
[22] El-Adawi MK, Abdel-Naby MA. Laser heating of a two-layer system with constant surface absorption: an exact solution. Int J Heat Mass Transfer 1995;38:947–52.
[23] Thomas LC. Heat transfer. Tulsa: Capstone Publishing Corporation; 1999.

[24] Zhao Z, Gold S, Poulikakos D. Pressure and power generation during explosive vaporization on a thin-film microheater. Int J Heat Mass Transfer 2000;43:218–96.
[25] Johnston RM, Brockett WA, Bock AE. Elements of applied thermodynamics. MD: Naval Institute Press; 1992.
[26] Kelly R, Miotello A. Comments on explosive mechanisms of laser sputtering. Appl Sur Sci 1996;96–98:205–15.
[27] Mark JE. Physical properties of polymers handbook. New York: AIP Press; 1996.